Received: 8 August 2023 | Revised: 11 October 2023 | Accepted: 27 October 2023

DOI: 10.1111/ppl.14078

SHORT COMMUNICATION

Physiologia Plantarum

Heterologous expression of *PtAAS1* reveals the metabolic potential of the common plant metabolite phenylacetaldehyde for auxin synthesis *in planta*

Jan Günther[1] | Rayko Halitschke[2] | Jonathan Gershenzon[1] | Meike Burow[3]

[1]Department for Biochemistry, Max Planck Institute for Chemical Ecology, Jena, Germany

[2]Department of Mass Spectrometry and Metabolomics, Max Planck Institute for Chemical Ecology, Jena, Germany

[3]Department of Plant and Environmental Sciences, University of Copenhagen, Frederiksberg C, Denmark

Correspondence
Jan Günther
Email: jg@plen.ku.dk

Funding information
Max-Planck-Gesellschaft; Novo Nordisk Fonden, Grant/Award Numbers: NNF20OC0060298, NNF20OC0065026

Edited by S. Martens

Abstract

Aromatic aldehydes and amines are common plant metabolites involved in several specialized metabolite biosynthesis pathways. Recently, we showed that the aromatic aldehyde synthase PtAAS1 and the aromatic amino acid decarboxylase PtAADC1 contribute to the herbivory-induced formation of volatile 2-phenylethanol and its glucoside 2-phenylethyl-β-D-glucopyranoside in *Populus trichocarpa*. To unravel alternative metabolic fates of phenylacetaldehyde and 2-phenylethylamine beyond alcohol and alcohol glucoside formation, we heterologously expressed *PtAAS1* and *PtAADC1* in *Nicotiana benthamiana* and analyzed plant extracts using untargeted LC-qTOF-MS and targeted LC–MS/MS analysis. While the metabolomes of *PtAADC1*-expressing plants did not significantly differ from those of control plants, expression of *PtAAS1* resulted in the accumulation of phenylacetic acid (PAA) and PAA-amino acid conjugates, identified as PAA-aspartate and PAA-glutamate. Herbivory-damaged poplar leaves revealed significantly induced accumulation of PAA-Asp, while levels of PAA remained unaltered upon herbivory. Transcriptome analysis showed that members of auxin-amido synthetase *GH3* genes involved in the conjugation of auxins with amino acids were significantly upregulated upon herbivory in *P. trichocarpa* leaves. Overall, our data indicates that phenylacetaldehyde generated by poplar PtAAS1 serves as a hub metabolite linking the biosynthesis of volatile, non-volatile herbivory-induced specialized metabolites, and phytohormones, suggesting that plant growth and defense can be balanced on a metabolic level.

1 | INTRODUCTION

Plant-specialized metabolites mediate plant responses to different biotic conditions and are generated by a plethora of biosynthetic pathways. These pathways can be initiated by key enzymes like cytochrome P450 enzymes (Irmisch et al., 2013; Sørensen et al., 2018), aminotransferases (Wang and Maeda, 2018), and group II pyridoxal phosphate (PLP)-dependent enzymes (Facchini et al., 2000). The latter comprise aromatic amino acid decarboxylase (AADC) and aromatic aldehyde synthase (AAS) enzymes that are involved in the biosynthesis of aromatic amino acid-derived specialized metabolites like benzylisoquinoline alkaloids (Facchini et al., 2000), monoterpene indole alkaloids (O'Connor and Maresh, 2006), hydroxycinnamic acid amides (Facchini et al., 2002), and phenylpropanoids in plants (Torrens-Spence et al., 2018; Günther et al., 2019). The floral volatile 2-phenylethanol is known to be emitted by flowers and fruits of many plant species, including roses and tomatoes (Tieman et al., 2006; Kaminaga et al., 2006). Other plant organs have been recently shown

to emit this volatile under various biotic conditions. For example, poplar trees under herbivore attack biosynthesize the volatile 2-phenylethanol and its glucoside 2-phenylethyl-β-D-glucopyranoside via separate biosynthetic pathways (Günther et al., 2019). This common volatile might serve to attract insects like parasitoid wasps or other herbivore predators as a form of indirect defense mechanism termed as a "cry for help" (Dicke and Baldwin, 2010). It has been shown previously that rose flowers emitting large amounts of volatile 2-phenylethanol accumulate the corresponding 2-phenylethyl-β-D-glucopyranoside (Watanabe et al., 2002). The formation of these metabolites can be initiated by the closely related group II PLP-dependent enzymes, PtAAS1 and PtAADC1. The direct reaction products of AAS and AADC enzymatic reactions, phenylacetaldehyde and 2-phenylethylamine, have been shown to respectively contribute to the biosynthesis of different plant metabolites (Sekimoto et al., 1998; Facchini et al., 2000; Facchini et al., 2002; Torrens-Spence et al., 2018). Previously, it has been shown that 2-phenylethylamine could be transformed to phenylacetaldehyde in subsequent biosynthetic steps in planta (Boatright et al., 2004; Tieman et al., 2006). The aromatic aldehyde phenylacetaldehyde has further been proposed to contribute to the biosynthesis of the auxin phenylacetic acid (Cook and Ross, 2016; Cook et al., 2016).

Auxins are plant hormones of paramount impact on plant development and growth. Although indole-3-acetic acid (IAA) is the most studied amongst this group of phytohormones, other natural auxins like phenylacetic acid (PAA), indole-3-butyric acid, indole-3-propionic acid and 4-chloroindole-3-acetic acid have been discovered (Abe et al., 1974; Fries and Iwasaki, 1976; Ludwig-Müller, 2011; Simon and Petrášek, 2011). Recent progress has led to an increased interest in the biosynthesis and physiology of the auxin PAA (Enders and Strader, 2016; Zhao, 2018). In comparison, IAA and PAA show distinctly different characteristics concerning their transport and distribution within the plant (Sugawara et al., 2015; Aoi et al., 2020). Both auxins target similar responsive elements, whereas a lower concentration of IAA compared to the concentration of PAA is sufficient to trigger these responses (Wightman and Lighty, 1982; Simon and Petrášek, 2011). Cellular concentrations of auxins are variable, and their developmental output is highly dependent on the local biosynthesis and local concentrations of these auxins (Wang et al., 2015; Zheng et al., 2016). Free auxin concentrations can be rapidly altered by auxin-amido synthetases belonging to the family GRETCHEN HAGEN 3 (GH3) (Westfall et al., 2016), which accept IAA as well as PAA and conjugate these substrates with different amino acids (Staswick et al., 2005; Sugawara et al., 2015). Conjugation has been shown to interfere with both signaling and transport of free auxins and thereby modulate signaling in plant development (Ljung et al., 2002; Ludwig-Müller, 2011; Zheng et al., 2016). Furthermore, specific fluctuations in auxin biosynthesis and transport trigger different developmental changes in the context of adaptation to stress (Grieneisen et al., 2007; Brumos et al., 2018; Zhao, 2018; Blakeslee et al., 2019). Generally, IAA and PAA can be biosynthesized via separate biosynthetic pathways within the plant kingdom (Pollmann et al., 2006; Mano and Nemoto, 2012; Zhao, 2014; Cook and Ross, 2016). To date, much is known about the biosynthetic pathways leading to the formation of IAA in *Arabidopsis thaliana* (Mashiguchi et al., 2011; Zhao, 2014; Enders and Strader, 2016). The initial steps of this biosynthetic network comprise the formation of indole-3-acetaldehyde and tryptamine (Figure S1; reviewed in Mano and Nemoto, 2012 and Zhao, 2014)). In further biosynthetic steps, these intermediates can be converted to the corresponding auxin IAA. Similarly, the biosynthesis of PAA can be initiated by separate pathways leading to the formation of phenylacetaldehyde (Kaminaga et al., 2006; Gutensohn et al., 2011; Günther et al., 2019) and 2-phenylethylamine (Tieman et al., 2006; Günther et al., 2019). In subsequent biosynthetic steps, these pathways might ultimately lead to the formation of PAA (Figure S2 and see Sekimoto et al., 1998).

In this study, we show that the key enzyme for the generation of the herbivory-induced metabolites phenylacetaldehyde, 2-phenylethanol and 2-phenylethyl-β-D-glucopyranoside in poplar leads to stimulated biosynthesis of the auxin PAA as well as PAA conjugates in planta.

2 | MATERIALS AND METHODS

2.1 | Plant material and treatment

Populus trichocarpa (genotype Muhle Larsen) trees were grown to a height of approximately 1 meter and *Lymantria dispar* herbivory was induced by subjecting 10 individuals (larval stage: L4) to the top part of the tree until the leaf 10 LPI. Therefore, young poplar trees were wrapped in polyethylene terephthalate bags ("Bratschlauch", Toppits) to enclose herbivores. After an incubation period overnight of 24 hours (start; 4:00 PM of day 1; end; 4:00 PM of day 2), herbivores were gently collected from the treated trees and all leaves (including midrib) and petiole were harvested ($n = 10$), flash frozen in nitrogen and stored at −80°C as described earlier (Günther et al., 2019). Agrobacterium-mediated expression of target genes in *N. benthamiana* was performed as described by Günther et al. (2019). Three days after transformation, plants were placed under mild direct light (LED 40%) for three more days. *N. benthamina* leaves, shoots and roots were harvested and processed ($n = 6$). Roots were cleared of soil by washing in a freshwater bath and dried with a paper towel. All plant samples were frozen in liquid nitrogen immediately after harvesting. Plant samples were stored at −80°C until further processing as described earlier (Günther et al., 2019).

2.2 | LC-qTOF-MS analysis of *N. benthamiana* methanol extracts

Methanol extracts (10:1 v/w) of *N. benthamiana* leaves were analyzed on an Ultimate 3000 UHPLC equipped with an Acclaim column (150 mm × 2.1 mm, particle size 2.2 µm) and connected to an IMPACT II UHR-Q-TOF-MS system (Bruker Daltonics) following a previously described program in positive and negative ionization mode (He et al., 2019). Raw data files were analyzed using Bruker Compass

DataAnalysis software version 4.3. Metabolomic differences of extracts were analyzed via MetaboScape 4.0 (Table S1). Furthermore, untargeted mass spectrometry (MS) data was normalized and visualized in volcano plots via XCMS (Tautenhahn et al., 2012; Gowda et al., 2014; Rinehart et al., 2014; Benton et al., 2015; Johnson et al., 2016).

2.3 | LC–MS/MS analysis of plant methanol extracts

Metabolites were extracted from ground plant material (*P. trichocarpa* or *N. benthamiana*) with methanol (10:1 v/w). Analytes were separated using an Agilent 1200 HPLC system on a Zorbax Eclipse XDB-C18 column (5034.6 mm, 1.8 µm; Agilent Technologies). HPLC parameters are given in Table S3. The HPLC was coupled to an API-6500 tandem mass spectrometer (Sciex) equipped with a turbospray ion source (ion spray voltage, 4500 eV; turbo gas temperature, 700°C; nebulizing gas, 60 p.s.i.; curtain gas, 40 p.s.i.; heating gas, 60 p.s.i.; collision gas, 2 p.s.i.). Multiple reaction monitoring (MRM) was used to monitor a parent ion → product ion reactions given in Table S4. The identification of PAA and IAA conjugates was performed according to LC–MS/MS fragmentation patterns as described in the following references (Irmisch et al., 2013; Sugawara et al., 2015; Westfall et al., 2016; Günther et al., 2018; Günther et al., 2019). Relative quantification was based on the relative abundance in measured extracts based on counts per second in standardized measurement conditions. Identification and quantification of PAA, 2-phenylethylamine, tyramine, tryptamine, 2-phenylethyl-β-D-glucopyranoside, tyrosine, tryptophan and phenylalanine were performed with authentic, commercially available standards (Table S5).

2.4 | Statistics

Statistical analysis was carried out as described in the figure legends. Student's t tests, Mann–Whitney Rank Sum tests, Kruskal-Wallis one-way analysis of variance (ANOVA), Dunn's tests and Tukey tests were performed with the software SigmaPlot 14.0 (Systat Software). EDGE tests for analysis of RNA-Seq datasets were performed with CLC Genomics Workbench (Qiagen Informatics) as described earlier (Günther et al., 2019).

2.5 | RNA extraction, cDNA synthesis and RNA-Seq analysis

Poplar leaf RNA extraction, cDNA synthesis and RNA-Seq analysis were carried out as described by Günther et al. (2019). For the identification of putative *Aux/IAA*, *GH3* and *SAUR* genes in the *P. trichocarpa* genome (Tuskan et al., 2006), the transcriptome annotations mapped to the poplar gene model version 3.0 provided by Phytozome (https://phytozome.jgi.doe.gov/pz/portal.html) were used for identification of members of the *Aux/IAA*, *GH3* and *SAUR* gene families. Candidates of the *Aux/IAA* and *GH3* gene family identified as herbivory-induced with above-average fold change and p-values below $p = 0.05$ were selected for visualization (Figures 3 and S9; Table S2). Total RPKM counts of all control and all herbivore-induced treatments were summed for the estimate of total transcript differences within the *SAUR* gene expression (Table S2).

2.6 | Phylogenetic analysis

Evolutionary analyses were conducted in MEGA X (Kumar et al., 2018). Coding sequences were retrieved from Phytozome (https://phytozome.jgi.doe.gov/pz/portal.html) and a multiple codon sequence alignment was performed via the guidance 2 server (Landan and Graur, 2008; Penn et al., 2010; Sela et al., 2015). The evolutionary history was inferred by using the Maximum Likelihood method based on the General Time Reversible model (Nei and Kumar, 2000). Initial trees were obtained automatically by applying Neighbor-Join and BioNJ algorithms to a matrix of pairwise distances estimated using the Maximum Composite Likelihood (MCL) approach, and then selecting the topology with superior log likelihood value. A discrete Gamma distribution was used to model evolutionary rate differences among sites (5 categories [+G, parameter = 1.5416]). The rate variation model allowed for sites to be evolutionarily invariable ([+I], 13.41% sites).

3 | RESULTS AND DISCUSSION

3.1 | Expression of *PtAAS1* and *PtAADC1* alters the accumulation of phenolic metabolites in *N. benthamiana*

We expressed *PtAAS1* and *PtAADC1* in leaves of *N. benthamiana* and quantified the aromatic amino acid substrates and aromatic amine products of AADC1 as well as the indirect reaction product of AAS1 (2-phenylethyl-β-D-glucopyranoside) via LC–MS/MS. As previously shown, levels of aromatic amines (Figure S3) and 2-phenylethyl-β-D-glucopyranoside (Figure S4) were increased upon *PtAADC1* and *PtAAS1* expression, respectively (Günther et al., 2019).

To investigate other potential metabolic alterations in *PtAAS1*- and *PtAADC1*-expressing *N. benthamiana* leaves, we performed untargeted LC-qTOF-MS analysis. The expression of *PtAAS1* and *PtAADC1* resulted in different metabolite profiles compared to wild type and *eGFP*-expressing control plants (Figure 1; Table S1). The expression of *PAADC1* and *PtAAS1* resulted in the differential accumulation of metabolites with a higher number of significantly up- or downregulated metabolites in the *PtAAS1*-expressing plants (Figure 1). Two candidate metabolites were exclusively present in *PtAAS1*-expressing lines and were identified as conjugates of phenylacetic acid with aspartate (PAA-Asp) and glutamate (PAA-Glu) via LC-qTOF-MS as described recently (Westfall et al., 2016; Aoi et al., 2020). Additionally, we observed characteristic insource fragmentation patterns of PAA-Asp and PAA-Glu in negative ionization mode, respectively (Figure S5). Several other phenolic compounds were detected but could not be identified based on the fragmentation pattern (Table S1).

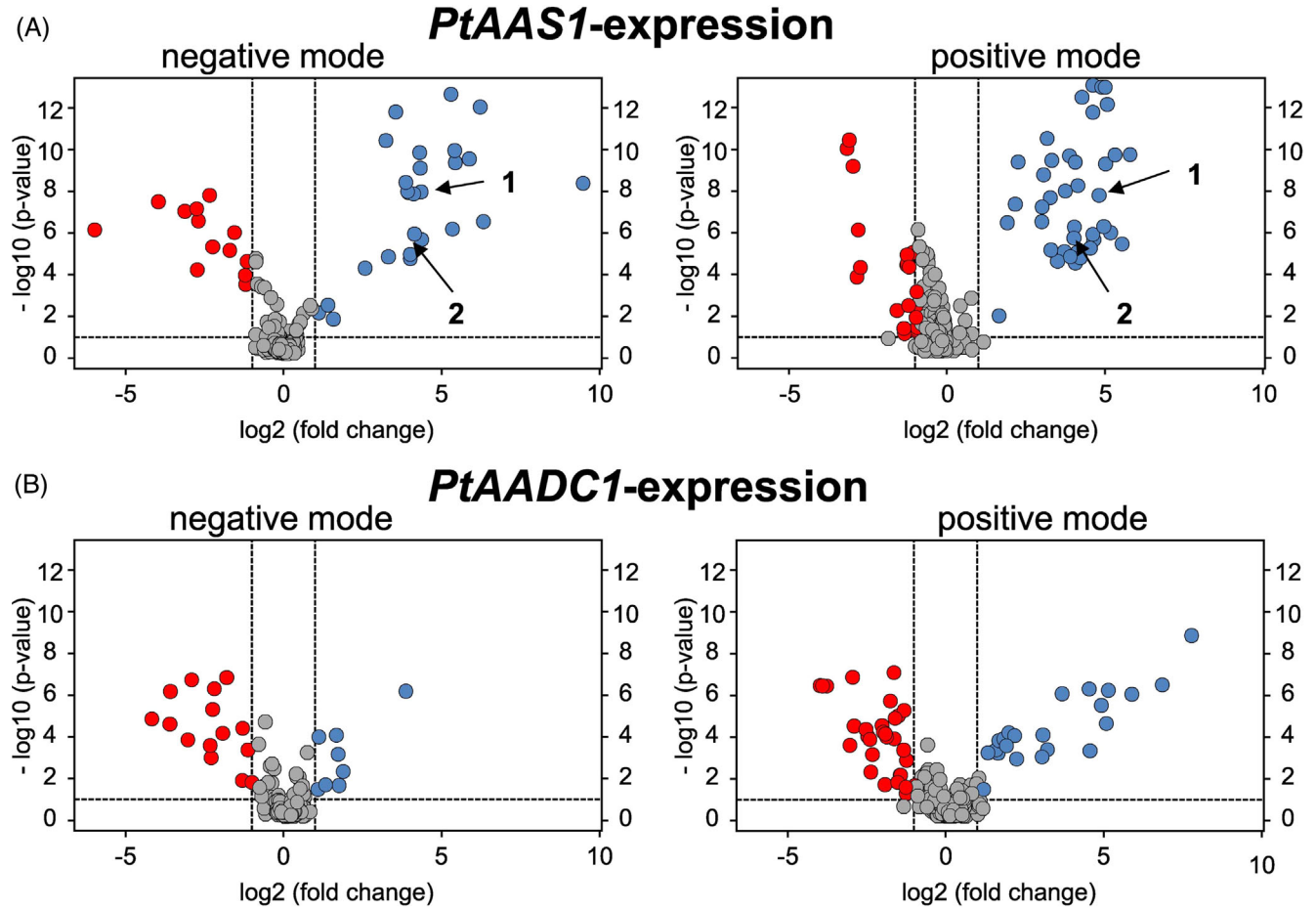

FIGURE 1 **Untargeted LC-qTOF-MS reveals significantly altered metabolites in *PtAAS1*-and *PtAADC1*-expressing *N. benthamiana* leaves.** Volcano plots of normalized LC-qToF-MS analysis of significantly upregulated (blue) and downregulated (red) metabolites in (A) *PtAAS1*- and (B) *PtAADC1*-expressing *N. benthamiana plants* in comparison to *eGFP*-expressing control plants (n = 6). PtAAS1-expression gives rise to PAA-Asp (compound 1) and PAA-Glu (compound 2), which are absent in the PtAADC1-expressing lines.

Expression of *PtAAS1* and the concomitant accumulation of auxin-conjugates pointed towards a conversion of the PtAAS1 reaction product phenylacetaldehyde to PAA-Asp and PAA-Glu in further metabolic steps in a heterologous plant system. It has been shown recently that aromatic aldehyde synthases generate aldehydes from corresponding aromatic amino acids and thereby initiate the formation of aromatic alcohols, alcohol glucosides (Torrens-Spence et al., 2018; Günther et al., 2019) and plant auxins (Sekimoto et al., 1998). Indeed, *PtAAS1*-expressing *N. benthamiana* plants also accumulated the auxin PAA in leaves (Figure 2). Despite the accumulation of PAA and conjugates in *N. benthaminana*, transient expression did not result in altered phenotypes in these plants. In comparison to reports in *Arabidopsis thaliana* rosette leaves, which were shown to contain up to 500 pmol/g fresh weight (~70 ng/g fresh weight) of endogenous PAA (Sugawara et al., 2015), the amounts of up to 700 ng/g fresh weight in leaves of *PtAAS1*-expressing *N. benthamiana* plants (Figure 2) are physiologically high. These high concentrations of the indirect PtAAS1 product PAA might have allowed highly promiscuous endogenous enzymes to accept this metabolite as a substrate (Moghe and Last, 2015). Such enzymes might be employed for detoxification of toxic intermediates within specialized metabolism (Sirikantaramas et al., 2008). Indeed, plant auxins can be inactivated via esterification with amino acids (Woodward and Bartel, 2005; Korasick et al., 2013). Taken together, our results in *N. benthamiana* illustrate that PtAAS1 activity can lead to the formation of the phenylalanine-derived auxin PAA in a heterologous plant system.

3.2 | Expression of phenylacetaldehyde-generating PtAAS1 leads to the accumulation of PAA- and IAA-conjugates in *N. benthamiana*

We further investigated the accumulation of PtAAS1-derived auxin metabolites in different tissues of *N. benthamiana* plants expressing *PtAAS1*. In order to further characterize the function of PtAAS1 and PtAADC1, we developed targeted analyses to quantify the reaction products and the auxin derivatives.

The auxin conjugates PAA-Asp and PAA-Glu accumulated in leaves and shoots (Figure 2). Furthermore, we detected these auxin conjugates in roots but their levels were not significantly increased in *PtAAS1*-expressing plants in comparison to wild type and *eGFP*-expression control plants (Figure S6). It has been reported that

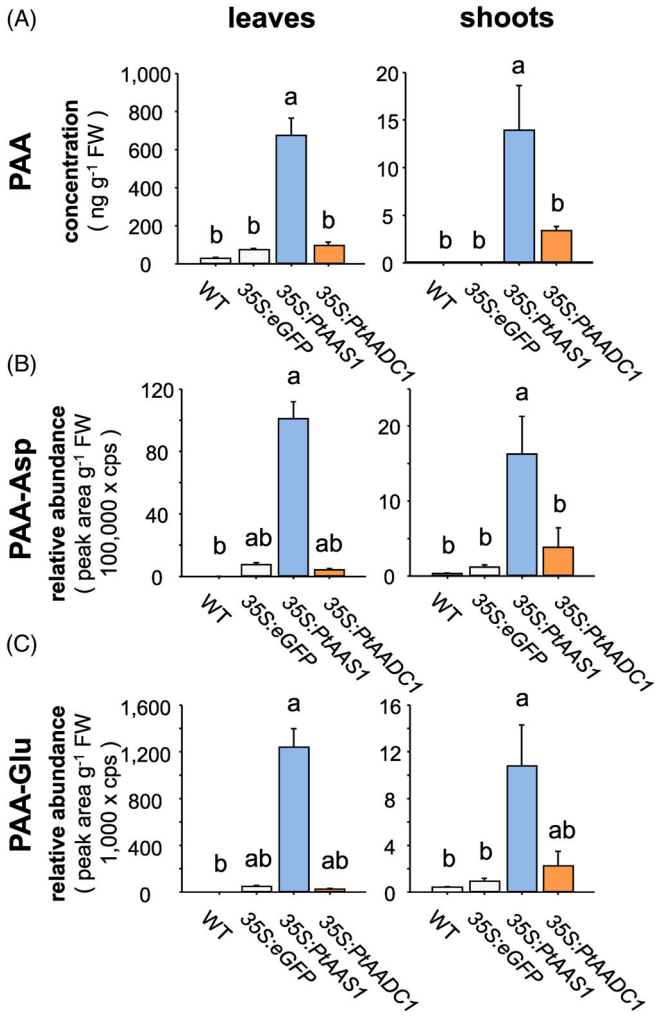

FIGURE 2 **Expression of *PtAAS1* results in increased levels of the auxin PAA, and its conjugates PAA-Asp and PAA-Glu in *N. benthamiana* leaves and shoots.** *N. benthamiana* leaves expressing poplar *PtAAS1* accumulate high amounts of (A) PAA, (B) PAA-Glu and (C) PAA-Asp in leaves and shoots. Different letters above each bar indicates statistically significant differences (Kruskal-Wallis One Way ANOVA) and are based on the following Tukey (shoots) or Dunn's test (leaves): PAA_{leaves} ($H = 19.607$, $P \leq 0.001$); PAA_{shoot} ($H = 12.275$, $P = 0.006$); $PAA\text{-}Asp_{leaves}$ ($H = 20.747$, $P \leq 0.001$); $PAA\text{-}Asp_{shoot}$ ($H = 19.127$, $P \leq 0.001$); $PAA\text{-}Glu_{leaves}$ ($H = 19.924$, $P \leq 0.001$); $PAA\text{-}Glu_{shoot}$ ($H = 15.647$, $P = 0.001$). Means + SE are shown ($n = 6$). FW, fresh weight.

A. thaliana plants with increased PAA biosynthesis also showed an increased accumulation of PAA-Asp, PAA-Glu and IAA-aspartate conjugate (IAA-Asp; Aoi et al., 2020). In line with these findings, we measured significantly increased levels of IAA-Asp in leaves and shoots of *PtAAS1*-expressing plants (Figure S7), highlighting that the increased auxin biosynthesis is accompanied by increased conversion of both auxins IAA and PAA into their respective conjugates (Mashiguchi et al., 2011; Sugawara et al., 2015; Aoi et al., 2020). Our results indicate that the expression of *PtAAS1* in *N. benthamiana* results in the increased biosynthesis of PAA and indicates that auxin conjugation with amino acids upon the increase of auxin biosynthesis or accumulation (Ludwig-Müller, 2011) might regulate the concentration of free, active auxin to mitigate the developmental effects of increased auxin biosynthesis (Zhao et al., 2001; Mashiguchi et al., 2011; Bunney et al., 2017). Furthermore, we could show that the PAA conjugates accumulate in the leaf tissue as well as in adjacent shoot and root tissues (Figures 2 and S6). These results allow for speculation of a directional transport of PAA conjugates biosynthesized in the leaves as reviewed recently (Leyser, 2018).

Plant auxins are involved in various stages of plant development and defense (Grieneisen et al., 2007; Brumos et al., 2018; Günther et al., 2018; Zhao, 2018; Blakeslee et al., 2019). Local auxin concentration is strictly regulated within plants via its transport, degradation and conjugation (Ljung et al., 2002; Staswick et al., 2005; Ludwig-Müller, 2011; Korasick et al., 2013; Sugawara et al., 2015; Zheng et al., 2016) and external application of auxins results in the increased accumulation of auxin conjugates. In this study, we induced high accumulation of the auxin PAA in a heterologous plant system via the expression of the phenylacetaldehyde-generating *PtAAS1* (Figures 1 and 2). The resulting accumulation of the corresponding PAA conjugates suggests that the pool size of free auxins is strictly regulated by conversion into inactive conjugates and possibly transport of these conjugates.

Taken together, *PtAAS1* contributes to the formation of PAA and PAA conjugates in planta. Additionally, as we also detected increased levels of IAA-Asp, our results provide evidence for the recently described crosstalk of PAA with IAA through coordinated conjugation of both free auxins (Aoi et al., 2020).

3.3 | The auxin conjugate PAA-Asp and putative *GH3* transcripts accumulate in herbivory-induced poplar leaves

We next tested whether herbivory-induced *P. trichocarpa* leaves with increased *PtAAS1* transcript levels show accumulation of PAA and PAA-Asp. We incubated *P. trichocarpa* trees with the herbivore *Lymantria dispar* caterpillars and quantified PAA and PAA-Asp in the leaves. Notably, the accumulation of PAA was unaltered in comparison to control leaves, whereas PAA-Asp was significantly increased upon herbivory (Figure 3). This suggests that, at the time point of harvest (24 hours after induction), PAA concentration had most likely returned to basal levels, whereas the level of the conjugation product was still increased.

It has been previously shown that increased auxin biosynthesis can be accompanied by the stimulated expression of auxin-responsive elements like *GH3* and *Aux/IAA* genes as well as the reduction of *SAUR* gene expression (Hagen and Guilfoyle, 2002). To evaluate whether transcripts of these gene families are upregulated in *P. trichocarpa* leaves challenged by herbivorous enemies, we screened for putative *Aux/IAA*, *GH3* and *SAUR* genes in our in-house transcriptome dataset. Amongst the family of 14 *GH3* genes identified in the poplar transcriptome, five candidates were significantly induced in response to herbivory (Figure 3). Phylogenetic relationship of these herbivory-induced transcript suggests that these genes might indeed encode GH3 enzymes that catalyze the conjugation of the auxin PAA with amino acids

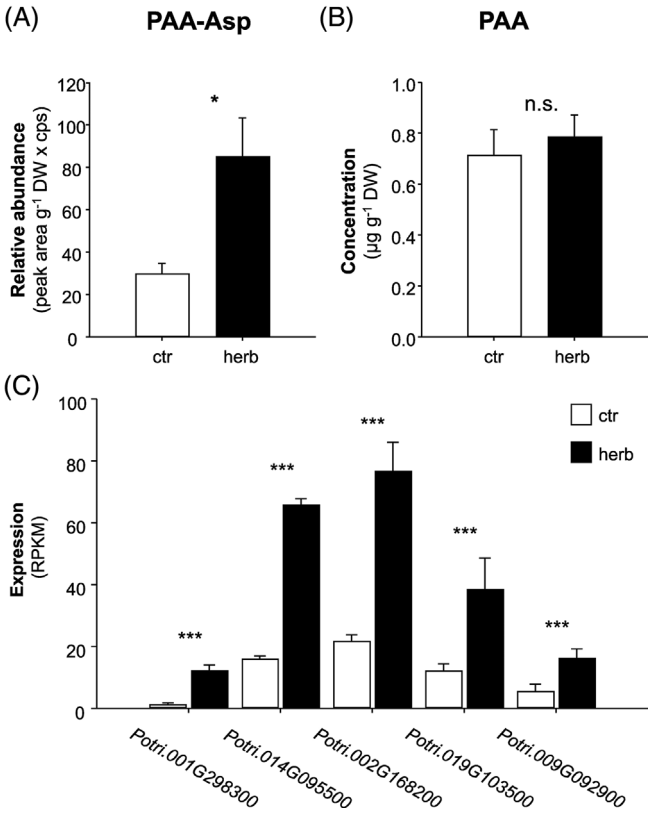

FIGURE 3 **Auxin, auxin conjugate and putative auxin-amido synthetase GH3 transcripts accumulate in herbivore-damaged leaves of *Populus trichocarpa*.** Accumulations of PAA-Asp (A) and phenylacetic acid (B), were analyzed in *L. dispar* damaged (herb) and undamaged control (ctr) leaves of *Populus trichocarpa* via LC–MS/MS. Asterisks indicate statistical significance in Student's t-test or in Mann–Whitney Rank Sum Tests. PAA ($P = 0.608$, $t = -0.522$); PAA-Asp ($P = 0.011$, $t = -2.816$). Putative auxin-amido synthetase *GH3* Gene expression (C) in herbivore-damaged and undamaged leaves was analyzed by Illumina HiSeq sequencing. Expression was normalized to RPKM. Significant differences in EDGE tests are visualized by asterisks. Means + SE are shown ($n = 4$). *Potri.001G298300* ($P = 2.22705E-10$, weighted difference (WD) = 1.71922E-05); *Potri.014G095500* ($P = 4.04229E-20$, WD = 7.9334E-05); *Potri.002G168200* ($P = 1.01033E-12$, WD = 8.83786E-05); *Potri.019G103500* ($P = 1.39832E-05$, WD = 4.27809E-05); *Potri.009G092900* ($P = 5.97467E-05$, WD = 1.72578E-05). Means + SE are shown ($n = 10$). DW, dry weight. n.s. – not significant.

(Figure S8; Staswick et al., 2005; Böttcher et al., 2011; Peat et al., 2012; Yu et al., 2018). The *Aux/IAA* gene family in poplar consists of 15 putative members, two of which were significantly upregulated in herbivory-induced poplar leaves (Figure S9). No transcripts of the 104-membered putative *SAUR* gene family were differentially expressed (Table S2). These results suggest that upon herbivory, putative *GH3* transcripts accumulate in poplar. The corresponding GH3 enzymes might lead to the formation of PAA-Asp in herbivory-induced poplar leaves.

Taken together, our results highlight a potential unprecedented role of PtAAS1 in the biosynthesis of the auxin PAA in planta. We hypothesize that the expression of *PtAAS1* in *N. benthamiana* leaves leads to an increased metabolic flow to generate high amounts of volatile 2-phenylethanol, 2-phenylethyl-β-D-glucopyranoside (Günther et al., 2019), PAA and PAA-conjugates in response to an increased biosynthesis of the hub metabolite phenylacetaldehyde.

Several studies revealed that the expression of key biosynthetic enzymes that initiate the biosynthesis of aromatic amino acid-derived specialized metabolites resulted in altered auxin phenotypes and chemotypes (Bak and Feyereisen, 2001; Bak et al., 2001; Irmisch et al., 2015; Günther et al., 2018; Perez et al., 2021; Perez et al., 2023). In Arabidopsis, another link between specialized metabolism and auxin signaling might be established by indole glucosinolate hydrolysis products with high affinity to the major auxin receptor TRANSPORT INHIBITOR RESPONSE 1 (TIR1), which could result in competitive binding and thereby feed into the auxin signaling cascade (Vik et al., 2018). Therefore, not only auxin but structural analogues, like indole glucosinolates and their hydrolysis products, might trigger auxin-induced developmental effects. Additionally, it has been recently reported that other non-aromatic glucosinolate catabolites are able to stimulate auxin-like phenotypes in Arabidopsis roots (Katz et al., 2015; Katz et al., 2020). Similarly, the maize defense compounds benzoxazolinones might contribute to auxin-induced growth through the interference with auxin perception (Hoshi-Sakoda et al., 1994), as maize CYP79A enzymes contribute to the formation of phenylalanine-derived defense compounds as well as to the formation of the corresponding auxin PAA in a heterologous plant system (Irmisch et al., 2015). Finally, a recent study of Aoi et al. (2020) showed that the expression of *CYP79A2* that leads to the formation of (*E*/*Z*)-phenylacetaldoxime in Arabidopsis resulted in effects similar to those of increased auxin biosynthesis and auxin conjugation.

Different pathways classified as specialized metabolism appear to have evolved to not only mediate plant biotic interactions but also provide regulatory input into auxin signaling. Increased expression of enzymes involved in the biosynthesis of amino acid-derived specialized metabolites might directly influence the homeostasis of the corresponding auxins. Additionally, by converging several separate biosynthetic paths leading to auxin, it is arguable whether the differential regulation of the individual pathways could concert a modular auxin response. This signal integration could potentially be defined by the flux through each individual pathway and only lead to activation of the auxin signaling cascade when the auxin pool reaches a specific threshold. This hypothesis has been appropriately termed "the bucket hypothesis" by Cook and Ross (2016). Assuming that auxin biosynthesis via phenylpyruvate is ubiquitous, biosynthesis via (*E*/*Z*)-pheylacetaldoxime and benzyl cyanide might be herbivore inducible. Yet, the latter would be metabolically more expensive as this pathway involves more reaction steps and nitrogen-containing intermediates (Neilson et al., 2013). In this perspective, the phenylethylamine pathway is moderately costly due to the comparably higher amount of biosynthetic enzymes involved in the pathway as well as the nitrogen-containing intermediate in comparison to the phenylpyruvate pathway (Figure 4). On the other hand, the pathway leading to phenylacetaldehyde via the aromatic aldehyde synthase releases nitrogen in the form of ammonium and progresses only via one

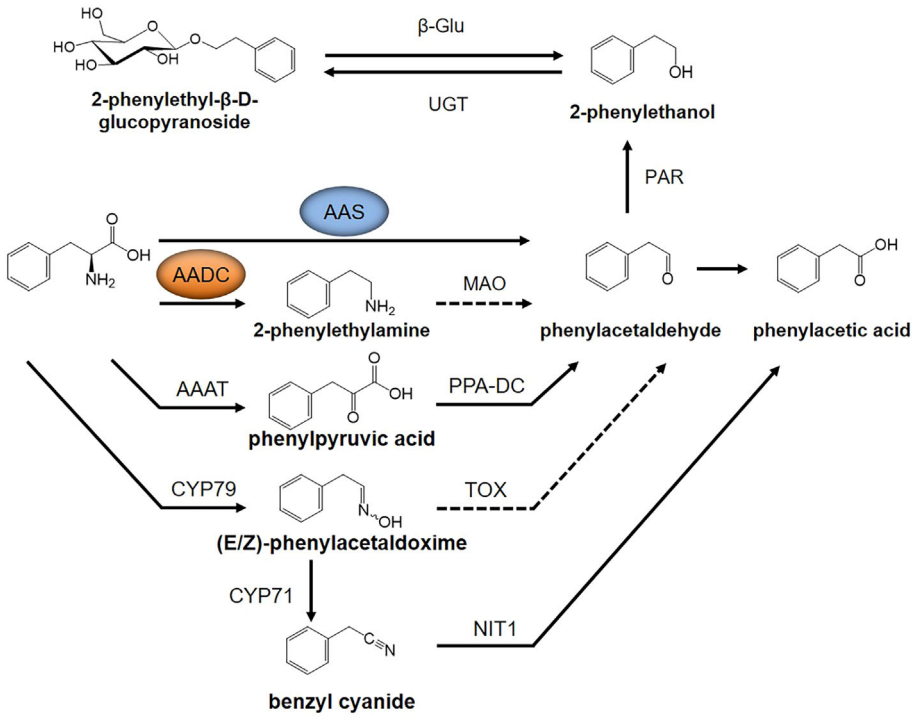

FIGURE 4 **Proposed pathways for the convergent biosynthesis of PAA in planta.** Convergent biosynthesis of PAA, phenylacetaldehyde and 2-phenylethanol can be initiated by AAS and AADC enzymes. The initiation of the formation of phenylacetaldehyde as a common substrate of 2-phenylethanol might also serve as substrate for the biosynthesis of the auxin PAA. Respective enzymes have been elucidated in planta. AAAT, aromatic amino acid transaminase; AADC, aromatic amino acid decarboxylase; CYP79, cytochrome P450 family 79 enzyme; PAAS, phenylacetaldehyde synthase; PPA-DC, phenylpyruvic acid decarboxylase; MAO, monoamine oxidase; TOX, transoximase; PAR, phenylacetaldehyde reductase; UGT, UDP-glucosyl transferase; β-Glu, β-glucosidase. Dashed line, enzymes not characterized in plants; solid line, enzymes characterized in plants.

enzyme that involves an enzymatic step and a non-enzymatic oxidation by molecular oxygen (Günther et al., 2019). From an enzyme kinetics perspective, a larger number of enzymes usually limits the potential flux through a pathway, resulting in a less rapid increase of the auxin pool. We propose that the aromatic aldehyde synthase pathway can provide the precursor, phenylacetaldehyde, at high metabolic flux and, therefore, rapidly generate auxin beyond the physiological threshold, resulting in the excitation of the auxin signaling cascade upon biotic stimuli. Future experiments need to be directed towards the measurements of the metabolic flux of the separate biosynthetic pathways as well as the transcriptional regulation of the corresponding biosynthetic enzymes leading to auxin in different plant species.

In summary, the poplar aromatic aldehyde synthase PtAAS1 contributes to the herbivory-induced formation of volatile 2-phenylethanol and 2-phenylethyl-β-D-glucopyranoside and additionally to the formation of the auxin PAA and auxin-derived conjugates in a heterologous plant system. We show that the conjugate of PAA-Asp accumulates upon herbivory in poplar leaves, suggesting that herbivory-induced expression of *PtAAS1* might contribute to PAA biosynthesis and might stimulate PAA signaling and metabolism in poplar. We conclude that the biosynthesis of the hub metabolite phenylacetaldehyde is of paramount importance for the generation of the auxin PAA and represents an additional pathway for the formation of the auxin PAA, expanding the metabolic network of the convergent biosynthesis of this auxin in planta (Figure 4). We unraveled unprecedented aspects of the biosynthesis of the auxin PAA in a heterologous plant system as well as in response to herbivory in *P. trichocarpa* leaves. Therefore, the phenylacetaldehyde hub metabolite represents a metabolic link between volatile, non-volatile herbivory-induced specialized metabolites, and phytohormones, suggesting that both growth and defense are balanced on a metabolic level (Erb and Kliebenstein, 2020). Further research should aim at elucidating and understanding the plant physiological responses following the increased PAA biosynthesis and conjugation upon herbivory.

AUTHOR CONTRIBUTIONS

J.Gü. and J.Ge. designed research. J.Gü., carried out the experimental work, analyzed data and wrote the manuscript. R.H. analyzed samples via untargeted LC-qToF-MS. J.Ge. and M.B. contributed to and finalized the manuscript. All authors read and approved the final manuscript.

ACKNOWLEDGMENTS

We appreciate the helpful comments and suggestions of Tobias G. Köllner on the manuscript. We thank Tamara Krügel, Danny Kessler, and all the MPI-CE gardeners for their help with rearing the poplar and *Nicotiana benthamiana* plants. D. Werck-Reichhart, Strasbourg, France, is thanked for kindly providing the pCAMBIA vectors and for the nice introduction to the USER cloning system. Open Access funding enabled and organized by Projekt DEAL.

FUNDING INFORMATION

The research was funded by the Max-Planck Society and Novo Nordisk Foundation grant No. (NNF20OC0065026 to M.B. and NNF20OC0060298 to J.G.).

DATA AVAILABILITY STATEMENT

Data sharing is not applicable to this article as all new created data is already contained within this article and the supplementals.

ORCID

Jan Günther https://orcid.org/0000-0001-8042-5241
Rayko Halitschke https://orcid.org/0000-0002-1109-8782
Jonathan Gershenzon https://orcid.org/0000-0002-1812-1551
Meike Burow https://orcid.org/0000-0002-2350-985X

REFERENCES

Abe, H., Uchiyama, M., and Sato, R. (1974). Isolation of phenylacetic acid and its *p*−hydroxy derivative as auxin-like substances from *Undaria pinnatifida*. *Agric. Biol. Chem.* 38:897–898.

Aoi, Y., Tanaka, K., Cook, S. D., Hayashi, K. I., and Kasahara, H. (2020). GH3 auxin-amido synthetases alter the ratio of indole-3-acetic acid and phenylacetic acid in Arabidopsis. *Plant Cell Physiol.* 61: 596–605.

Bak, S., and Feyereisen, R. (2001). The Involvement of Two P450 Enzymes, CYP83B1 and CYP83A1, in Auxin Homeostasis and Glucosinolate Biosynthesis. *Plant Physiol.* 127:108–118.

Bak, S., Tax, F. E., Feldmann, K. A., Galbraith, D. W., and Feyereisen, R. (2001). CYP83B1, a Cytochrome P450 at the Metabolic Branch Point in Auxin and Indole Glucosinolate Biosynthesis in Arabidopsis. *Plant Cell Online* 13:101–111.

Benton, H. P., Ivanisevic, J., Mahieu, N. G., Kurczy, M. E., Johnson, C. H., Franco, L., Rinehart, D., Valentine, E., Gowda, H., Ubhi, B. K., et al. (2015). Autonomous metabolomics for rapid metabolite identification in global profiling. *Anal. Chem.* 87:884–891.

Blakeslee, J. J., Spatola Rossi, T., Kriechbaumer, V., and Raines, C. (2019). Auxin biosynthesis: Spatial regulation and adaptation to stress. *J. Exp. Bot.* 70:5041–5049.

Boatright, J., Negre, F., Chen, X., Kish, C. M., Wood, B., Peel, G., Orlova, I., Gang, D., Rhodes, D., and Dudareva, N. (2004). Understanding in Vivo Benzenoid Metabolism in Petunia Petal Tissue. *Plant Physiol.* 135: 1993–2011.

Böttcher, C., Boss, P. K., and Davies, C. (2011). Acyl substrate preferences of an IAA-amido synthetase account for variations in grape (*Vitis vinifera* L.) berry ripening caused by different auxinic compounds indicating the importance of auxin conjugation in plant development. *J. Exp. Bot.* 62:4267–4280.

Brumos, J., Robles, L. M., Yun, J., Vu, T. C., Jackson, S., Alonso, J. M., Stepanova, A. N., Brumos, J., Robles, L. M., Yun, J., et al. (2018). Local Auxin Biosynthesis Is a Key Regulator of Plant Article Local Auxin Biosynthesis Is a Key Regulator of Plant Development. *Dev. Cell* 47:306-318.e5.

Bunney, P. E., Zink, A. N., Holm, A. A., Billington, C. J., and Kotz, C. M. (2017). Local auxin metabolism regulates environment-induced hypocotyl elongation. *Physiol. Behav.* 176:139–148.

Cook, S. D., and Ross, J. J. (2016). The auxins, IAA and PAA, are synthesized by similar steps catalyzed by different enzymes. *Plant Signal. Behav.* 11:1–4.

Cook, S. D., Nichols, D. S., Smith, J., Chourey, P. S., McAdam, E. L., Quittenden, L., and Ross, J. J. (2016). Auxin Biosynthesis: Are the Indole-3-Acetic Acid and Phenylacetic Acid Biosynthesis Pathways Mirror Images? *Plant Physiol.* 171:1230–41.

Dicke, M., and Baldwin, I. T. (2010). The evolutionary context for herbivore-induced plant volatiles: beyond the "cry for help." *Trends Plant Sci.* 15:167–175.

Enders, T. A., and Strader, L. C. (2016). Auxin Activity: Past, present, and Future. *Am. J. Bot.* 102:180–196.

Erb, M., and Kliebenstein, D. J. (2020). Plant Secondary Metabolites as Defenses, Regulators, and Primary Metabolites: The Blurred Functional Trichotomy1[OPEN]. *Plant Physiol.* 184:39–52.

Facchini, P. J., Huber-Allanach, K. L., and Tari, L. W. (2000). Plant aromatic L-amino acid decarboxylases: Evolution, biochemistry, regulation, and metabolic engineering applications. *Phytochemistry* 54: 121–138.

Facchini, P. J., Hagel, J., and Zulak, K. G. (2002). Hydroxycinnamic acid amide metabolism: physiology and biochemistry. *Can. J. Bot.* 80: 577–589.

Fries, L., and Iwasaki, H. (1976). p-Hydroxyphenylacetic acid and other phenolic compounds as growth stimulators of the red alga *Porphyra tenera*. *Plant Sci. Lett.* 6:299–307.

Gowda, H., Ivanisevic, J., Johnson, C. H., Kurczy, M. E., Benton, H. P., Rinehart, D., Nguyen, T., Ray, J., Kuehl, J., Arevalo, B., et al. (2014). Interactive XCMS online: Simplifying advanced metabolomic data processing and subsequent statistical analyses. *Anal. Chem.* 86:6931–6939.

Grieneisen, V. A., Xu, J., Marée, A. F. M., Hogeweg, P., and Scheres, B. (2007). Auxin transport is sufficient to generate a maximum and gradient guiding root growth. *Nature* 449:1008–1013.

Günther, J., Irmisch, S., Lackus, N. D., Reichelt, M., Gershenzon, J., and Köllner, T. G. (2018). The nitrilase PtNIT1 catabolizes herbivore-induced nitriles in *Populus trichocarpa*. *BMC Plant Biol.* 18:1–12.

Günther, J., Lackus, N. D., Schmidt, A., Huber, M., Stödler, H.-J., Reichelt, M., Gershenzon, J., and Köllner, T. G. (2019). Separate pathways contribute to the herbivore-induced formation of 2-phenylethanol in poplar. *Plant Physiol.* 180:767–782.

Gutensohn, M., Klempien, A., Kaminaga, Y., Nagegowda, D. A., Negre-Zakharov, F., Huh, J. H., Luo, H., Weizbauer, R., Mengiste, T., Tholl, D., et al. (2011). Role of aromatic aldehyde synthase in wounding/herbivory response and flower scent production in different Arabidopsis ecotypes. *Plant J.* 66:591–602.

Hagen, G., and Guilfoyle, T. (2002). Auxin-responsive gene expression : genes, promoters and regulatory factors. *Plant Mol. Biol.* 49:373–385.

He, J., Fandino, R. A., Halitschke, R., Luck, K., Köllner, T. G., Murdock, M. H., Ray, R., Gase, K., Knaden, M., Baldwin, I. T., et al. (2019). An unbiased approach elucidates variation in (S)-(+)-linalool, a context-specific mediator of a tri-trophic interaction in wild tobacco. *Proc. Natl. Acad. Sci. U. S. A.* 116:14651–14660.

Hoshi-Sakoda, M., Usui, K., Ishizuka, K., Kosemura, S., Yamamura, S., and Hasegawa, K. (1994). Structure-activity relationships of benzoxazolinones with respect to auxin-induced growth and auxin-binding protein. *Phytochemistry* 37:297–300.

Irmisch, S., Clavijo McCormick, A., Boeckler, G. A., Schmidt, A., Reichelt, M., Schneider, B., Block, K., Schnitzler, J.-P., Gershenzon, J., Unsicker, S. B., et al. (2013). Two Herbivore-Induced Cytochrome P450 Enzymes CYP79D6 and CYP79D7 Catalyze the Formation of Volatile Aldoximes Involved in Poplar Defense. *Plant Cell* 25:4737–4754.

Irmisch, S., Zeltner, P., Handrick, V., Gershenzon, J., and Köllner, T. G. (2015). The maize cytochrome P450 CYP79A61 produces phenylacetaldoxime and indole-3-acetaldoxime in heterologous systems and might contribute to plant defense and auxin formation. *BMC Plant Biol.* 15:128.

Johnson, C. H., Ivanisevic, J., and Siuzdak, G. (2016). Metabolomics: beyond biomarkers and towards mechanisms. *Nat. Rev. Mol. Cell Biol.* 17:451–459.

Kaminaga, Y., Schnepp, J., Peel, G., Kish, C. M., Ben-Nissan, G., Weiss, D., Orlova, I., Lavie, O., Rhodes, D., Wood, K., et al. (2006). Plant phenylacetaldehyde synthase is a bifunctional homotetrameric enzyme that catalyzes phenylalanine decarboxylation and oxidation. *J. Biol. Chem.* 281:23357–23366.

Katz, E., Nisani, S., Yadav, B. S., Woldemariam, M. G., Shai, B., Obolski, U., Ehrlich, M., Shani, E., Jander, G., and Chamovitz, D. A. (2015). The glucosinolate breakdown product indole-3-carbinol acts as an auxin antagonist in roots of *Arabidopsis thaliana*. *Plant J.* 82: 547–555.

Katz, E., Bagchi, R., Jeschke, V., Rasmussen, A. R. M., Hopper, A., Burow, M., Estelle, M., and Kliebenstein, D. J. (2020). Diverse allyl glucosinolate catabolites independently influence root growth and development. *Plant Physiol.* 183:1376–1390.

Korasick, D. A., Enders, T. A., and Strader, L. C. (2013). Auxin biosynthesis and storage forms. *J. Exp. Bot.* 64:2541–2555.

Kumar, S., Stecher, G., Li, M., Knyaz, C., and Tamura, K. (2018). MEGA X: Molecular evolutionary genetics analysis across computing platforms. *Mol. Biol. Evol.* 35:1547–1549.

Landan, G., and Graur, D. (2008). Local reliability measures from sets of co-optimal multiple sequence alignments. *Pacific Symp. Biocomput.* 13: 15–24.

Leyser, O. (2018). Auxin signaling. *Plant Physiol.* 176:465–479.

Ljung, K., Hull, A. K., Kowalczyk, M., Marchant, A., Celenza, J., Cohen, J. D., and Sandberg, G. (2002). Biosynthesis, conjugation, catabolism and homeostasis of indole-3-acetic acid in *Arabidopsis thaliana*. *Plant Mol. Biol.* 50:309–332.

Ludwig-Müller, J. (2011). Auxin conjugates: Their role for plant development and in the evolution of land plants. *J. Exp. Bot.* 62: 1757–1773.

Mano, Y., and Nemoto, K. (2012). The pathway of auxin biosynthesis in plants. *J. Exp. Bot.* 63:2853–2872.

Mashiguchi, K., Tanaka, K., Sakai, T., Sugawara, S., Kawaide, H., Natsume, M., Hanada, A., Yaeno, T., Shirasu, K., Yao, H., et al. (2011). The main auxin biosynthesis pathway in *Arabidopsis*. *Proc. Natl. Acad. Sci.* 108:18512–18517.

Moghe, G., and Last, R. L. (2015). Something old, something new: Conserved enzymes and the evolution of novelty in plant specialized metabolism. *Plant Physiol.* 169:pp.00994.2015.

Nei, M., and Kumar, S. (2000). *Molecular evolution and phylogenetics*. Oxford university press.

Neilson, E. H., Goodger, J. Q. D., Woodrow, I. E., and Møller, B. L. (2013). Plant chemical defense: At what cost? *Trends Plant Sci.* 18:250–258.

O'Connor, S. E., and Maresh, J. J. (2006). Chemistry and biology of monoterpene indole alkaloid biosynthesis. *Nat. Prod. Rep.* 23:532–547.

Peat, T. S., Böttcher, C., Newman, J., Lucent, D., Cowieson, N., and Davies, C. (2012). Crystal structure of an indole-3-acetic acid amido synthetase from grapevine involved in auxin homeostasis. *Plant Cell* 24:4525–4538.

Penn, O., Privman, E., Ashkenazy, H., Landan, G., Graur, D., and Pupko, T. (2010). GUIDANCE: A web server for assessing alignment confidence scores. *Nucleic Acids Res.* 38:23–28.

Perez, V. C., Dai, R., Bai, B., Tomiczek, B., Askey, B. C., Zhang, Y., Rubin, G. M., Ding, Y., Grenning, A., Block, A. K., et al. (2021). Aldoximes are precursors of auxins in Arabidopsis and maize. *New Phytol.* 231:1449–1461.

Perez, V. C., Dai, R., Tomiczek, B., Mendoza, J., Wolf, E. S. A., Grenning, A., Vermerris, W., Block, A. K., and Kim, J. (2023). Metabolic link between auxin production and specialized metabolites in Sorghum bicolor. *J. Exp. Bot.* 74:364–376.

Pollmann, S., Müller, A., and Weiler, E. W. (2006). Many roads lead to "auxin": Of nitrilases, synthases, and amidases. *Plant Biol.* 8:326–333.

Rinehart, D., Johnson, C. H., Nguyen, T., Ivanisevic, J., Benton, H. P., Lloyd, J., Arkin, A. P., Deutschbauer, A. M., Patti, G. J., and Siuzdak, G. (2014). Metabolomic data streaming for biology-dependent data acquisition. *Nat. Biotechnol.* 32:524–527.

Sekimoto, H., Seo, M., Kawakami, N., Komano, T., Desloire, S., Liotenberg, S., Marion-Poll, A., Caboche, M., Kamiya, Y., and Koshiba, T. (1998). Molecular cloning and characterization of aldehyde oxidases in *Arabidopsis thaliana*. *Plant Cell Physiol.* 39:433–442.

Sela, I., Ashkenazy, H., Katoh, K., and Pupko, T. (2015). GUIDANCE2: Accurate detection of unreliable alignment regions accounting for the uncertainty of multiple parameters. *Nucleic Acids Res.* 43:W7–W14.

Simon, S., and Petrášek, J. (2011). Why plants need more than one type of auxin. *Plant Sci.* 180:454–460.

Sirikantaramas, S., Yamazaki, M., and Saito, K. (2008). Mechanisms of resistance to self-produced toxic secondary metabolites in plants. *Phytochem. Rev.* 7:467–477.

Sørensen, M., Neilson, E. H. J., and Møller, B. L. (2018). Oximes : Unrecognized Chameleons in General and Specialized Plant Metabolism. *Mol. Plant* 11:95–117.

Staswick, P. E., Serban, B., Rowe, M., Tiryaki, I., Maldonado, M. T., Maldonado, M. C., and Suza, W. (2005). Characterization of an Arabidopsis Enzyme Family That Conjugates Amino Acids to Indole-3-Acetic Acid. *Plant Cell* 17:616–627.

Sugawara, S., Mashiguchi, K., Tanaka, K., Hishiyama, S., Sakai, T., Hanada, K., Kinoshita-Tsujimura, K., Yu, H., Dai, X., Takebayashi, Y., et al. (2015). Distinct Characteristics of Indole-3-Acetic Acid and Phenylacetic Acid, Two Common Auxins in Plants. *Plant Cell Physiol.* 56: 1641–1654.

Tautenhahn, R., Cho, K., Uritboonthai, W., Zhu, Z., Patti, G. J., and Siuzdak, G. (2012). An accelerated workflow for untargeted metabolomics using the METLIN database. *Nat. Biotechnol.* 30: 826–828.

Tieman, D., Taylor, M., Schauer, N., Fernie, A. R., Hanson, A. D., and Klee, H. J. (2006). Tomato aromatic amino acid decarboxylases participate in synthesis of the flavor volatiles 2-phenylethanol and 2-phenylacetaldehyde. *Proc. Natl. Acad. Sci.* 103:8287–8292.

Torrens-Spence, M. P., Pluskal, T., Li, F. S., Carballo, V., and Weng, J. K. (2018). Complete Pathway Elucidation and Heterologous Reconstitution of Rhodiola Salidroside Biosynthesis. *Mol. Plant* 11:205–217.

Tuskan, G. A., DiFazio, S., Jansson, S., Bohlmann, J., Grigoriev, I., Hellsten, U., Putnam, N., Ralph, S., Rombauts, S., Salamov, A., et al. (2006). The Genome of Black Cottonwood, *Populus trichocarpa* (Torr. & Gray). *Science.* 313:1596–1604.

Vik, D., Mitarai, N., Wulff, N., Halkier, B. A., and Burow, M. (2018). Dynamic modeling of indole glucosinolate hydrolysis and its impact on auxin signaling. *Front. Plant Sci.* 9:1–16.

Wang, M., and Maeda, H. A. (2018). Aromatic amino acid aminotransferases in plants. *Phytochem. Rev.* 17:131–159.

Wang, B., Chu, J., Yu, T., Xu, Q., Sun, X., Yuan, J., Xiong, G., Wang, G., Wang, Y., and Li, J. (2015). Tryptophan-independent auxin biosynthesis contributes to early embryogenesis in *Arabidopsis*. *Proc. Natl. Acad. Sci.* 112:4821–4826.

Watanabe, S., Hayashi, K., Yagi, K., Asai, T., MacTavish, H., Picone, J., Turnbull, C., and Watanabe, N. (2002). Biogenesis of 2-Phenylethanol in Rose Flowers: Incorporation of [$^2H_8$]L-Phenylalanine into 2-Phenylethanol and its β-D-Glucopyranoside during the Flower Opening of *Rosa* `Hoh-Jun' and *Rosa damascena* Mill.; *Biosci. Biotechnol. Biochem.* 66:943–947.

Westfall, C. S., Sherp, A. M., Zubieta, C., Alvarez, S., Schraft, E., Marcellin, R., Ramirez, L., and Jez, J. M. (2016). *Arabidopsis thaliana* GH3.5 acyl acid amido synthetase mediates metabolic crosstalk in auxin and salicylic acid homeostasis. *Proc. Natl. Acad. Sci.* 113:13917–13922.

Wightman, F., and Lighty, D. L. (1982). Identification of phenylacetic acid as a natural auxin in the shoots of higher plants. *Physiol. Plant.* 55: 17–24.

Woodward, A. W., and Bartel, B. (2005). Auxin: Regulation, action, and interaction. *Ann. Bot.* 95:707–735.

Yu, D., Qanmber, G., Lu, L., Wang, L., Li, J., Yang, Z., Liu, Z., Li, Y., Chen, Q., Mendu, V., et al. (2018). Genome-wide analysis of cotton GH3 subfamily II reveals functional divergence in fiber development, hormone response and plant architecture. *BMC Plant Biol.* 18.

Zhao, Y. (2014). Auxin Biosynthesis. *Arab. B.* 12:e0173.

Zhao, Y. (2018). Essential Roles of Local Auxin Biosynthesis in Plant Development and in Adaptation to Environmental Changes. *Annu. Rev. Plant Biol.* 69:417–435.

Zhao, Y., Christensen, S. K., Fankhauser, C., Cashman, J. R., Cohen, J. D., Weigel, D., and Chory, J. (2001). A role for flavin monooxygenase-like enzymes in auxin biosynthesis. *Science.* 291:306–309.

Zheng, Z., Guo, Y., Novák, O., Chen, W., Ljung, K., Noel, J. P., and Chory, J. (2016). Local auxin metabolism regulates environmentinduced hypocotyl elongation. *Nat. Plants* 2:1–9.

SUPPORTING INFORMATION

Additional supporting information can be found online in the Supporting Information section at the end of this article.

How to cite this article: Günther, J., Halitschke, R., Gershenzon, J. & Burow, M. (2023) Heterologous expression of *PtAAS1* reveals the metabolic potential of the common plant metabolite phenylacetaldehyde for auxin synthesis *in planta*. *Physiologia Plantarum*, 175(6), e14078. Available from: https://doi.org/10.1111/ppl.14078